JACC Vol. 30, No. 7
December 1997:1625–32

Dissociation Between Changes in Intramyocardial Function and Left Ventricular Volumes in the Eight Weeks After First Anterior Myocardial Infarction

CHRISTOPHER M. KRAMER, MD, FACC, WALTER J. ROGERS, MS, THERESE M. THEOBALD, MPH, THOMAS P. POWER, MD, GENNADY GESKIN, MD, NATHANIEL REICHEK, MD, FACC

Pittsburgh, Pennsylvania

Objectives. **We sought to examine the relation between regional changes in intramyocardial function and global left ventricular (LV) remodeling in the first 8 weeks after reperfused first anterior myocardial infarction (MI).**

Background. **Because of limitations in imaging methods used to date, this relation has not been thoroughly evaluated.**

Methods. **We studied 26 patients (21 men, 5 women; mean age 51 years) by magnetic resonance imaging (MRI) on day 5 ± 2 (mean ± SD) and week 8 ± 1 after their first anterior MI. All patients had single-vessel left anterior descending coronary artery disease and although they had received reperfusion therapy, all had regional LV dysfunction and an initial ejection fraction (EF) ≤50%. Short-axis magnetic resonance tagging was performed spanning the LV. Percent intramyocardial circumferential shortening (%S) on a topographic basis, LV mass index, LV end-diastolic volume index (LVEDVI), LV end-systolic volume index and LV ejection fraction (LVEF) were measured.**

Results. **Left ventricular mass index tended to decrease, whereas the LVEDVI increased from 82 ± 24 to 96 ± 27 ml/m^2 ($p = 0.002$). Left ventricular end-systolic volume index remained unchanged, whereas LVEF increased from 39 ± 12% to 45 ± 14% ($p = 0.002$). Apical %S improved from 9 ± 6% to 13 ± 5% ($p < 0.0001$), as it did in the midanterior (6 ± 6% to 10 ± 7%, $p < 0.02$) and midseptal regions (8 ± 7% to 12 ± 6%, $p < 0.02$). Early dysfunction in remote midinferior and basal lateral regions resolved by 8 weeks. By multivariate analysis, the only significant predictor of an increase in LVEDVI over the study period was peak creatine kinase ($p = 0.04$).**

Conclusions. **In the first 8 weeks after a large, reperfused anterior MI, %S improved in the apex, midanterior and midseptal regions and normalized in remote noninfarct-related regions, but LV end-diastolic volumes also increased. This increased LVEDVI correlated with infarct size by peak creatine kinase and was not related to changes in global and regional LV function.**

(J Am Coll Cardiol 1997;30:1625–32)

The hallmark of left ventricular (LV) remodeling after myocardial infarction (MI) is LV dilation (1,2). The initial event is expansion of the infarct-related segment (3,4) due to cell slippage (5), followed by lengthening of noninfarct-related segments (6,7) due to cell slippage and cellular hypertrophy (8,9). The natural history of regional intramyocardial function in the chronic phase after nonreperfused MI has been studied in an ovine model (7) using magnetic resonance tagging (10,11). In this model, LV dilation and hypertrophy progress despite an improvement in function in regions adjacent to the infarct-related segment over time. In humans, we have recently demonstrated dysfunction in remote noninfarct-related regions early after reperfused anterior MI using magnetic resonance tagging (12). The relation between changes in intramyocardial function over time and changes in LV volumes and mass in humans is not fully understood.

The end result of LV remodeling is an increase in end-diastolic and end-systolic volumes, which is predictive of increased mortality after MI (13). In the past decade, therapies to limit LV remodeling have been developed(14) and demonstrated to limit mortality after large MI with LV dysfunction (15–17). We wished to examine the relation between intramyocardial function and LV remodeling after anterior MI in this era to better understand correlates of the remodeling process.

Methods

Patient group. This study was approved by the Institutional Review Board of Allegheny General Hospital, and all human subjects gave written informed consent. Ten normal subjects, including seven men and three women (mean age 42 ± 15 years), underwent magnetic resonance imaging (MRI). None had clinical or echocardiographic evidence of cardiac disease.

From the Division of Cardiology, Department of Medicine, Allegheny University of the Health Sciences, Allegheny Campus, Pittsburgh, Pennsylvania. This study was supported by a grant from the Allegheny University of the Health Sciences, Pittsburgh, Pennsylvania.

Manuscript received April 4, 1997; revised manuscript received August 15, 1997, accepted August 25, 1997.

Address for correspondence: Dr. Christopher M. Kramer, Cardiology Division, Allegheny General Hospital, 320 East North Avenue, Pittsburgh, Pennsylvania 15212. E-mail: ckramer@pgh.auhs.edu.

Published by Elsevier Science Inc.

0735-1097/97/$17.00
PII S0735-1097(97)00406-3

Abbreviations and Acronyms

ACE = angiotensin-converting enzyme
LAD = left anterior descending coronary artery
LV = left ventricle, left ventricular
LVEDVI = left ventricular end-diastolic volume index
LVEF = left ventricular ejection fraction
LVESVI = left ventricular end-systolic volume index
LVMI = left ventricular mass index
MI = myocardial infarction
MRI = magnetic resonance imaging
%S = percent intramyocardial circumferential shortening

We initially studied 32 patients after their first anterior MI. All had left anterior descending coronary artery (LAD) single-vessel disease without significant (≥50%) disease in the other major epicardial coronary arteries. The diagnosis of MI was made in the conventional manner using clinical history, electrocardiography and plasma creatine kinase levels, drawn every 8 h and elevated to more than twice the normal level with an MB fraction >5%.

All patients were studied by MRI on day 5 ± 2 after MI. One patient died suddenly at home on day 10 after MI; two patients underwent single-vessel coronary artery bypass graft surgery within the first few weeks after MI for significant proximal LAD disease; and three patients did not return for follow-up. The remaining 26 patients returned for repeat MRI at 8 ± 1 weeks after MI and comprise the study group (Table 1).

The average age of the 26 patients was 51 ± 12 years; 21 were men and 5 were women. Three were treated with thrombolysis alone, 16 with primary angioplasty and 7 with rescue angioplasty after failed thrombolytic therapy. The average time to reperfusion in the 23 patients for which this variable was known was 307 ± 166 min. The peak creatine kinase level was 2,861 ± 1,917 U/liter. By electrocardiography, 21 patients had Q wave and 5 had non–Q wave infarctions. All had evidence of regional LV dysfunction and an LV ejection fraction (LVEF) ≤50% by left ventriculography or echocardiography before entry into the study. The mean LVEF by these imaging techniques was 38 ± 8%. All had a documented patent infarct-related artery and Thrombolysis in Myocardial Infarction flow grade 3 by X-ray angiography before the initial study. The patients' medications between day 5 and week 8 included aspirin in 21 patients, angiotensin-converting enzyme (ACE) inhibitors in 21, beta-blockers in 17, Coumadin in 15, nitrates in 4, digoxin in 3, lasix in 1 and a calcium channel blocker in 1.

Table 1. Clinical Variables in the 26 Study Patients

					First MRI		Second MRI				
Pt No./ Gender	Age (yr)	Rx	Time to Rx (min)	Peak CK (U/liter)	HR (beats/min)	BP (mm Hg)	HR (beats/min)	BP (mm Hg)	ACE	Beta-Blocker	Nitrates
1/M	42	t-PA/PTCA	270	1,300	100	134/80	92	128/74	Y	Y	N
2/M	37	PTCA	N/A	4,310	86	110/70	60	96/60	Y	Y	N
3/M	72	t-PA/PTCA	335	2,370	68	112/64	68	100/60	Y	Y	N
4/M	53	t-PA/PTCA	85	7,470	78	100/66	76	90/60	Y	N	N
5/M	46	PTCA	225	3,870	87	100/70	67	100/72	Y	N	Y
6/F	53	PTCA	658	1,426	63	96/60	70		Y	N	N
7/M	78	t-PA/PTCA	195	1,208	76	130/70	56	150/76	Y	Y	N
8/M	51	PTCA	90	2,185	68	98/60	56	110/70	N	Y	Y
9/M	43	t-PA	90	4,932	84	110/70	67	118/70	Y	N	N
10/M	65	PTCA	178	3,580	63	110/60	60	120/64	Y	N	N
11/F	61	t-PA	360	4,925	115	119/79	125	130/90	Y	Y	N
12/M	57	PTCA	255	1,894	68	102/63	64	147/88	Y	Y	N
13/M	33	PTCA	215	5,505	75	125/76	80	110/66	N	Y	N
14/M	63	t-PA	N/A	2,838	81	98/60	77	118/78	Y	Y	Y
15/M	52	PTCA	200	1,137	71	138/78	57	123/73	Y	Y	N
16/M	44	t-PA/PTCA	450	2,123	103	107/67	80	110/70	Y	Y	N
17/M	45	PTCA	189	4,080	83	111/74	73	106/70	Y	N	N
18/M	60	PTCA	280	2,385	94	105/63	94	100/80	Y	N	Y
19/M	53	PTCA	580	1,845	66	93/64	63	101/79	Y	N	N
20/F	56	PTCA	185	963	81	91/51	61	91/59	N	Y	N
21/M	39	t-PA/PTCA	410	6,770	83	100/64	64	102/34	Y	N	N
22/M	64	PTCA	93	2,404	72	132/84	84	116/73	Y	Y	N
23/M	36	PTCA	471	426	79	124/67	51	124/67	N	Y	N
24/F	45	PTCA	418	909	77	105/65	100	160/109	Y	Y	N
25/M	38	t-PA/PTCA	220	3,940	75	102/61	66	127/70	Y	Y	N
26/F	48	PTCA	122	1,211	62	102/69	51	145/101	N	Y	N

ACE = angiotensin-converting enzyme inhibitor; BP = blood pressure; CK = creatine kinase; F = female; HR = heart rate; M = male; MRI = magnetic resonance image; N = no; N/A = not available; Pt = patient; PTCA = percutaneous transluminal coronary angioplasty; Rx = treatment; t-PA = tissue-type plasminogen activator; Y = yes.

MRI. MRI was performed with a Siemens Magnetom SP 1.5-T scanner with the patient prone on an elliptical spine surface coil with electrocardiographic monitoring and gating. The imaging protocol has been well described previously (12). Briefly, localizing scout images were followed by a single short-axis cine series in a plane near the mitral valve, which provided images every 40 ms to identify end-systole as the point of minimal LV cavity area. Then a series of short-axis, single-slice, multiple cardiac phase, tagged images were obtained using a breath-hold, gradient echo method with a segmented k-space acquisition. Tag stripe separation was 7 mm; field of view was 280 mm; and matrix size was 128 × 256, interpolated to 256 × 256 for display, yielding a pixel size of 1.09 × 1.09 mm. Repetition time (TR), which determined the temporal resolution, was adjusted (from a minimum of 58 ms to a maximum of 90 ms) so as to time one image of the five-phase image series at end-systole (always either the fourth or fifth image). Each breath-hold spanned 18 heartbeats or 14 to 15 s/breath-hold at the average heart rate of the patients during the two studies. Seven-millimeter thick, contiguous image planes or slices were generated (Fig. 1), enough to span the entire LV cavity from base to apex. The entire imaging session lasted ~45 min. The identical imaging protocol was performed for the 8-week post-MI study. The same number of slices, on average, were acquired in the two studies (n = 12 ± 1 for both).

Data analysis. Quantitative analysis of images was performed by a single investigator (T.M.T.) who had no knowledge of the clinical information, using an operator-driven image analysis tool developed in the "Volumetric Image Display and Analysis" software package (VIDA, University of Iowa) loaded on a Sun workstation. Left ventricular mass was calculated from planimetered epicardial and endocardial areas of interleaved short-axis end-diastolic images according to previously published techniques (7,12) and was indexed to body surface area. Left ventricular end-diastolic volume index (LVEDVI), left ventricular end-systolic volume index (LVESVI) and LVEF were calculated using planimetered end-diastolic and end-systolic areas in the same manner.

Quantitative analysis of shortening was performed using an operator-driven, interstripe-distance measuring software tool developed in VIDA, as well as previously published methods (7,12). Percent intramyocardial circumferential shortening (%S) was measured at endocardial, mid-wall and epicardial sites in the anterior, lateral, septal and inferior regions in the LV short-axis in all of the slices from apex to base in each study. The total number of slices along the long axis of the ventricle was divided into apical, midventricular and basal thirds (four slices each on average), and data from these slices were averaged. A total of 12 LV regions were thereby evaluated.

Statistical methods. Clinical variables, including heart rate, blood pressure, left ventricular mass index (LVMI), LVEDVI, LVESVI, LVEF and regional %S were compared between the day 5 and week 8 studies by the Student paired *t* test. Regional %S was compared in patients on day 5 and at week 8 after MI with that of normal subjects using unpaired *t* test. Stepwise multivariate regression analysis was performed to assess correlates of the increase in LVEDVI from day 5 to week 8 and the increase in LVEF during the same period.

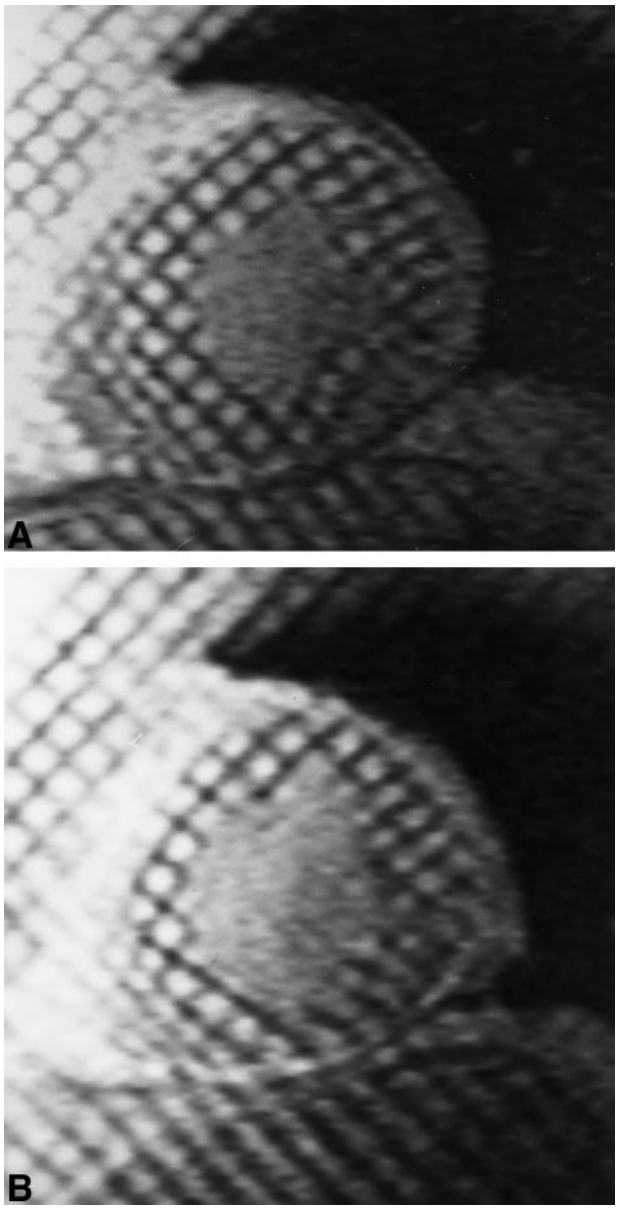

Figure 1. A, End-systolic apical magnetic resonance-tagged short-axis image in a patient on day 4 after anterior MI. The right ventricular apex and interventricular septum are in the 6 to 9 o'clock position on the image; the anterior wall from 9 to 12 o'clock; the lateral wall from 12 to 3 o'clock; and the inferior wall from 3 to 6 o'clock. Reduced deformation of the tag stripes is seen in the anterior wall and septum relative to the lateral and inferior regions. **B,** End-systolic apical magnetic resonance-tagged short-axis image in the same patient, now 8 weeks after anterior MI. The image orientation and apex to base position are the same as in **A**. Note the thinning of the anterior wall and septum, the continued lack of deformation in those regions and the preserved deformation in the lateral and inferior walls. The end-systolic LV cavity area is clearly larger here than on the day 4 image.

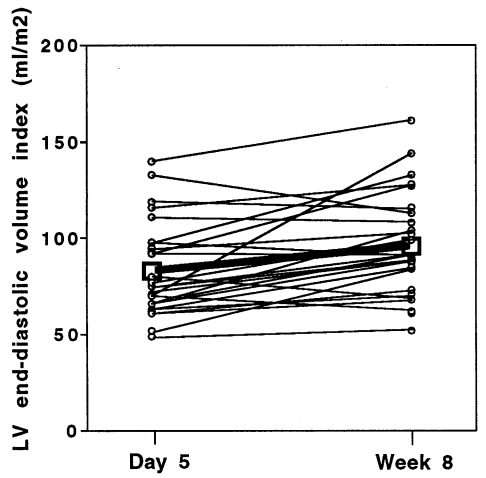

Figure 2. Graph demonstrating the change in LVEDVI from the day 5 to week 8 study in each of the 26 patients. **Large open squares** = mean value.

Variables included in the analysis were age, gender, time to reperfusion, peak creatine kinase, LVMI, LVEDVI and LVESVI on day 5; %S at the LV apex and %S at the LV base on day 5; endocardial %S throughout the heart on day 5; ACE inhibitor therapy; and beta-blocker therapy. All results are expressed as mean value ± SD. A p value <0.05 was considered statistically significant.

Results

Clinical findings. The patients' heart rate during MRI on day 5 after MI was 80 ± 13 beats/min, and their systolic and diastolic blood pressures were 110 ± 14 mm Hg and 68 ± 7 mm Hg, respectively. During MRI at week 8 after MI, the average heart rate was 73 ± 17 beats/min ($p < 0.02$ vs. week 1), whereas the average blood pressures were not significantly different (systolic 118 ± 20 mm Hg, $p = 0.07$; diastolic 73 ± 16 mm Hg, $p = 0.14$).

LV global variables. The LVMI tended to decrease during the 8-week period, falling from 109 ± 19 to 102 ± 18 g/m^2 ($p = 0.075$). The LVEDVI increased from 83 ± 24 to 96 ± 27 ml/m^2 ($p = 0.002$) (Fig. 2), whereas the LVESVI did not change (52 ± 20 ml/m^2 on day 5 to 54 ± 24 ml/m^2 at week 8, $p = 0.42$). LVEF increased during this period from 39 ± 12% to 45 ± 14% ($p = 0.002$). Therefore, despite a significant increase in LVEDVI, global LV function improved in the 8-week post-MI period.

Regional intramyocardial function. Percent S in the 12 regions around the LV from the MRI studies in the normal subjects and in the patients on day 5 and at week 8 after MI is shown in Table 2. When data from the three transmural levels were averaged (Table 2, Fig. 3), a significant improvement in %S was seen throughout all regions within the apex, as apical anterior %S improved from 4 ± 6% to 7 ± 8% ($p < 0.04$), apical septal %S increased from 4 ± 6% to 8 ± 6% ($p = 0.002$), apical inferior %S increased from 14 ± 10% to 18 ± 9% ($p = 0.004$) and apical lateral %S increased from 15 ± 9% to 18 ± 8% ($p < 0.04$). Other regions that demonstrated improvement included the midseptum from 8 ± 7% to 12 ±

Table 2. Regional Intramyocardial Percent Circumferential Shortening in Normal Subjects and in Patients at Day 5 and Week 8 After Anterior Myocardial Infarction

	Endocardial	Mid	Epicardial	Average
Apex				
Anterior				
Normal	24 ± 5	23 ± 4	19 ± 6	22 ± 4
Day 5	7 ± 9*	3 ± 7*	2 ± 5*	4 ± 6*
Week 8	8 ± 10*	7 ± 8*	6 ± 7*†	7 ± 8*†
Septum				
Normal	28 ± 4	22 ± 4	17 ± 4	23 ± 3
Day 5	5 ± 7*	4 ± 6*	3 ± 8*	4 ± 6*
Week 8	11 ± 7*†	7 ± 6*†	7 ± 7*†	8 ± 6*†
Inferior				
Normal	24 ± 8	22 ± 5	18 ± 5	21 ± 5
Day 5	16 ± 10*	13 ± 9*	13 ± 10*	14 ± 10*
Week 8	21 ± 8†	17 ± 9*†	15 ± 10	18 ± 9†
Lateral				
Normal	35 ± 4	27 ± 6	23 ± 4	28 ± 4
Day 5	16 ± 9*	15 ± 9*	17 ± 8*	15 ± 9*
Week 8	19 ± 10*	18 ± 8*	13 ± 9*	18 ± 8*†
Mid				
Anterior				
Normal	22 ± 12	20 ± 5	14 ± 4	18 ± 6
Day 5	9 ± 7*	5 ± 7*	5 ± 5*	6 ± 6*
Week 8	12 ± 9*†	9 ± 8*†	9 ± 8*†	10 ± 7*†
Septum				
Normal	25 ± 4	22 ± 6	16 ± 5	21 ± 4
Day 5	10 ± 8*	8 ± 9*	7 ± 7*	8 ± 7*
Week 8	14 ± 8*†	11 ± 8*	9 ± 7*	12 ± 6*†
Inferior				
Normal	25 ± 5	20 ± 5	17 ± 4	21 ± 4
Day 5	17 ± 14*	15 ± 11	13 ± 12	15 ± 11*
Week 8	21 ± 7	17 ± 7	15 ± 7	18 ± 6
Lateral				
Normal	31 ± 5	26 ± 5	23 ± 5	27 ± 2
Day 5	17 ± 9*	18 ± 7*	13 ± 6*	16 ± 7*
Week 8	19 ± 9*	20 ± 8*	16 ± 7*†	18 ± 7*
Base				
Anterior				
Normal	19 ± 4	16 ± 3	13 ± 5	16 ± 3
Day 5	14 ± 8*	10 ± 7*	7 ± 8*	11 ± 6*
Week 8	15 ± 8	12 ± 6*	10 ± 7	13 ± 6*
Septum				
Normal	23 ± 3	20 ± 4	16 ± 5	19 ± 4
Day 5	18 ± 9*	13 ± 8*	13 ± 8*	15 ± 7*
Week 8	18 ± 9*	14 ± 4*	11 ± 5*	14 ± 4*
Inferior				
Normal	22 ± 6	17 ± 4	13 ± 7	17 ± 5
Day 5	21 ± 9	19 ± 8	16 ± 7	19 ± 8
Week 8	21 ± 8	19 ± 6	16 ± 5	19 ± 6
Lateral				
Normal	27 ± 7	21 ± 9	19 ± 9	23 ± 7
Day 5	22 ± 7*	19 ± 6	14 ± 8	18 ± 5*
Week 8	24 ± 7	21 ± 6	18 ± 5†	21 ± 5†

*$p < 0.05$ versus normal subjects. †$p < 0.05$ versus day 5. Data presented are mean value ± SD.

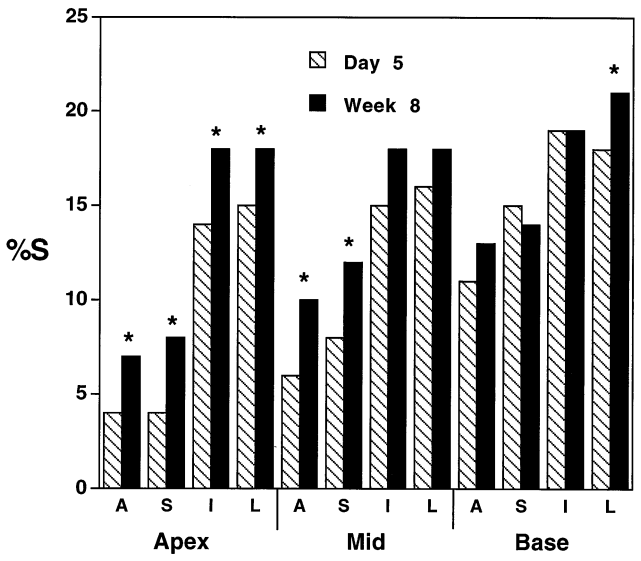

Figure 3. Percent circumferential intramyocardial shortening (%S) by short-axis and long-axis locations in patients on day 5 **(striped bars)** and at week 8 **(solid bars)** after anterior MI when values from all transmural sites are averaged. A = anterior; I = inferior; L = lateral; S = septal. *$p < 0.05$ versus day 5.

6% ($p < 0.02$), the midanterior wall from 6 ± 6% to 10 ± 7% ($p < 0.02$) and the basal lateral wall from 18 ± 5% to 21 ± 5% ($p < 0.05$).

Resolution of dysfunction in patients as compared with normal subjects from day 5 to week 8 was seen in the apical inferior, midinferior and basal lateral regions (Table 2). The last two regions are remote from infarct-related territory (12).

When data from all three transmural locations and four sites around the short axis were averaged, significant improvement was noted in the apex and midventricle over the 8-week period after MI. Apical %S improved from 9 ± 6% to 13 ± 5% ($p < 0.0001$) and midventricular %S from 11 ± 5% to 14 ± 5% ($p = 0.001$), although %S in both regions in patients remained less than that in normal subjects (24 ± 3% and 22 ± 3%, respectively, $p < 0.001$). No significant increase was found in basal %S (from 15 ± 4% on day 5 to 17 ± 3% at week 8, $p = 0.24$), although by 8 weeks basal %S was no longer different from that of normal subjects (19 ± 3%, $p = 0.11$).

When values from three transmural sites and all slices from apex to base were averaged, significant improvement in %S was seen in all regions around the short axis of the ventricle between the two studies. Septal %S increased from 9 ± 5% to 11 ± 5% ($p < 0.02$), anterior %S from 7 ± 5% to 10 ± 6% ($p < 0.02$), lateral %S from 16 ± 6% to 19 ± 5% ($p < 0.01$) and inferior %S from 16 ± 8% to 18 ± 6% ($p < 0.04$). Only the inferior wall demonstrated normal %S, both on day 5 and at week 8 after MI.

Predictors of LV remodeling. Stepwise multivariate regression analysis for the change in LVEDVI from day 5 to week 8 after MI demonstrated that the only significant predictor was peak creatine kinase (ΔLVEDVI = 0.004 × Peak creatine kinase + 1.30, $p < 0.05$, $r = 0.43$). Lower %S at the LV base on day 5 after MI showed a trend toward predicting a change in LVEDVI ($p = 0.09$). Variables that were not significantly associated with an increase in LVEDVI were age ($p = 0.85$), male gender ($p = 0.28$), time to reperfusion ($p = 0.75$), ACE inhibitor ($p = 0.59$) or beta-blocker therapy ($p = 0.44$), LVMI ($p = 0.25$), LVEDVI ($p = 0.22$), LVESVI ($p = 0.99$), apical %S ($p = 0.92$) and endocardial %S throughout the heart ($p = 0.66$). No independent predictors of improvement in LVEF from the day 5 to week 8 study were found.

Discussion

This study demonstrated that in the 8 weeks after a large anterior MI in 26 patients with single-vessel LAD disease, regional intramyocardial function improved within all of the apical regions as well as the midanterior, midseptal and basal lateral regions. Dysfunction in remote noninfarct-related regions, including the midinferior and basal lateral regions (12), resolved in the later post-MI period. Despite the improvement in regional intramyocardial function, the LV dilated with a mean increase in end-diastolic volume of 13 ml/m^2, or 16%, although global LV function improved with an increase in the EF from 39 ± 12% to 45 ± 14%. The only significant predictor of the increase in LVEDVI was peak creatine kinase as a measure of infarct size. Percent S at the LV base on day 5, a marker of remote region dysfunction, tended to predict increased LVEDVI.

Previous animal studies. In an ovine model of nonreperfused anteroapical infarction, we found no improvement in function within the infarct zone over a 6-month period, most likely due to its transmural nature (7). Using radiopaque markers in a pig model of infarction, Holmes et al. (18) demonstrated an absence of systolic segment shortening in the infarct zone 3 weeks after MI. In accordance with the present study, our ovine study demonstrated a trend toward improvement in %S from week 1 to week 8 after MI in adjacent and remote noninfarct-related regions (7). Despite improved regional function, LV dilation progressed in this model.

Previous human studies. Imaging modalities used previously to study LV remodeling (6,19,20) have not allowed evaluation of intramyocardial function. However, Picard et al. (19) demonstrated by two-dimensional echocardiography that the amount of dysfunctional endocardial surface area indexed to body size increases over a 3-month period after nonreperfused anterior MI, mostly due to infarct expansion at the apex. These patients developed global LV dilation in an era before the use of ACE inhibitors. Other investigators have shown improvement in regional function in reperfused infarction with echocardiographic techniques (21,22). Hirose et al. (23) demonstrated by serial cine computed tomographic scanning after MI that intrinsic LV contractile performance did not change as estimated by a fall in the rate-corrected velocity of circumferential fiber shortening, which was termed an appropriate response to increased LV end-systolic wall stress.

Using radionuclide angiography, Jeremy et al. (24) demonstrated that of 50 patients with a first MI, 21 (42%) demon-

strated an increase of end-diastolic volume by >20% over a 6-month period. Eight of these 21 patients dilated progressively on serial examinations and all eight had anterior infarctions. Serial cine computed tomographic scanning in patients after the initial transmural anterior MI and in patients with patent infarct-related arteries, before ACE inhibitors were used routinely (25), has shown that the LV end-diastolic volume increased 22%, from 148 ± 8 to 180 ± 9 ml during the first year after MI, whereas LV mass tended to decrease in the first 6 weeks, consistent with the present study. Approximately 40% of the increase in LV end-diastolic volume occurred in the first 9 weeks. In mid-ventricular echocardiographic images from the Survival and Ventricular Enlargement (SAVE) study, the percent change in LV cavity area at 1 year was 27% in the treated group and 29% in the nontreated groups (20). Another study using quantitative echocardiography over the course of a year after anterior and inferior MI (26) showed no increase in end-systolic volumes and an improvement in LVEF, similar to the findings of the present study.

Potential mechanisms. Several potential mechanisms may explain improved function in the apex and midanterior and midseptal regions. For one, these regions are heterogeneous, likely representing a mix of infarct-related and adjacent noninfarct-related tissue, and for that reason, demonstrate some residual %S on day 5. The improvement may primarily occur within islands of noninfarct-related myocardium adjacent to infarct-related myocardium (7). Improved %S may also represent resolution of stunning (27) due in part to successful reperfusion (21,22) and the effects of ACE inhibitors (20,28), with which the majority of patients were treated. Resolution of the dysfunction in remote noninfarct-related regions may be due to a reduction in tethering effects as the mechanical function of more apical regions improve, or to improvement in blood flow reserve in these regions (29). Reduced end-systolic wall stress (30) is an unlikely mechanism of improved function as end-systolic volume and systolic blood pressure were unchanged and LV mass tended to decrease.

Potential mechanisms for the continued increase in end-diastolic volume despite improved regional function include expansion of the infarct-related territory (2,3,18,19) and cell slippage in infarct-related and noninfarct-related regions (5,31). Elevated mechanical load has been postulated as a stimulus to remodeling (6,7), as has neurohumoral stimulation, which has been associated with increased cardiovascular mortality and heart failure (32). ACE inhibition is known to limit but not prevent increases in end-diastolic volume over time (20,28).

Correlates of LV remodeling. A study by Gaudron et al. (33) of 70 patients after their first MI identified several factors by multivariate analysis that were predictors of remodeling over a 3-year period. Predictors in their study included initial LVEF and stroke index, ventriculographic infarct size, infarct location (anterior) and TIMI flow grade infarct-related artery perfusion. In the present study, all of the infarcts were anterior and demonstrated Thrombolysis in Myocardial Infarction flow grade 3. Peak creatine kinase, as a marker of infarct size, was an important predictor. Apical %S, as a marker of infarct region function, did not correlate with remodeling, likely due to the uniformity of dysfunction within the infarct-related region. Endocardial %S within the whole heart by magnetic resonance tagging on day 5 was not predictive of remodeling and may not correlate closely to absolute infarct size owing to the presence of dysfunctional myocardium that later improves. However, %S at the base on day 5, representative of dysfunction in regions remote from the infarct, tended to have predictive value.

Studies in the rat model have demonstrated that the degree of LV remodeling (34) and mortality after MI (14) are linearly related to infarct size. Using technetium-99m sestamibi imaging to define infarct size in humans, investigators at the Mayo Clinic (35) showed a close correlation between infarct size and changes over the first year after MI in end-systolic volume ($r = 0.63$) and LVEF ($r = -0.66$) in a patient group with a documented patent infarct-related artery.

Study limitations. One limitation of the study is the size of the study group. Certainly, a larger patient study group would improve the power of the study to identify predictors of the remodeling process. Nonetheless, the patient group is homogeneous (all had reperfused anterior MI with single-vessel LAD disease) and MRI data on changes in LV volumes are reproducible (36). The homogeneity of the patient group precludes the extrapolation of these data to patients with inferior infarction, previous infarction, multivessel disease or nonreperfused infarction.

Ensuring that %S is measured in the same regions in the two studies is a potential pitfall. However, this problem was alleviated by measuring %S in each slice from apex to base and dividing the ventricle into apical, mid and basal thirds. This could lead to small potential errors in matching regions, in that remodeling is characterized by lengthening of noninfarct-related regions over time (6,7). However, the same number of 7-mm thick slices were imaged on the day 5 and week 8 studies ($n = 12 \pm 1$ vs. $n = 12 \pm 1$, p = NS).

Values for %S may be heart rate–dependent over wide ranges of changes. A modest fall in heart rate was noted between the two studies (80 ± 13 beats/min on day 5 vs. 73 ± 17 beats/min at week 8 [$p < 0.02$]) and might explain part of the improvement in %S over time. There were 11 patients whose heart rate fell by >10 beats/min. However, there was no significant difference between this group and the group of 15 patients whose heart rate did not fall by >10 beats/min in the increase in %S from day 5 to week 8 averaged for the whole heart (4 ± 2% for those with a heart rate decrease >10 beats/min vs. 2 ± 3% for the others, $p = 0.14$).

The only significant predictor of change in LVEDVI over time was peak creatine kinase as a reasonable estimate of infarct size. Creatine kinase has been used for nearly three decades for infarct sizing (37,38) but has known limitations in the reperfusion era (39). All the patients in this study had regional ventricular dysfunction at study entry and were reperfused on average >5 h after chest pain onset, which may

enhance the ability to use peak creatine kinase as a measure of infarct size.

The patients did not uniformly have assessment of the patency of the infarct-related artery at the time of the 8-week study, although all arteries were patent on day 5 and there were no documented interval events in the study group. A subgroup of 14 patients did have assessment of patency by MRI coronary angiography (40), and of those, 13 had flow visualized within the LAD. The beneficial effect of infarct-related artery patency on LV remodeling and prognosis after acute MI is now well established (41,42). Reocclusion without reinfarction can lead to increased remodeling (43).

Types but not doses of medications were recorded at the time of MRI at 8 weeks after MI. The doses of ACE inhibitors and beta-blockers may have been increased slightly between day 5 and hospital discharge. Recent data suggest that higher doses of ACE inhibitors have more favorable effects on LV size and function early after MI (44). Higher doses of ACE inhibitors might have limited the increase in LVEDVI seen in this study.

Conclusions. In the first 8 weeks after large reperfused first anterior MI, intramyocardial function improved in the apex and mid-anteroseptum, dysfunction resolved in remote noninfarct-related regions and LVEF rose. However, LV end-diastolic volumes increased despite improvement in function during this period. The increase in LVEDVI correlated with infarct size by creatine kinase and was not related to changes in global and regional LV function.

We gratefully acknowledge the patient recruitment efforts of Susan Petruolo, RN, and the support of the magnetic resonance imaging technologists at Allegheny General Hospital, especially June Yamrozik and Lois Miller.

References

1. McKay RG, Pfeffer MA, Pasternak RC, et al. Left ventricular remodeling following myocardial infarction: a corollary to infarct expansion. Circulation 1986;74:693–702.
2. Eaton LW, Weiss JL, Bulkley BH, Garrison JB, Weisfeldt MD. Regional cardiac dilatation after acute myocardial infarction. N Engl J Med 1979;300: 57–62.
3. Erlebacher JA, Weiss JL, Eaton LW, Kallman C, Weisfeldt ML, Buckley BH. Late effects of acute infarct dilation on heart size: a two dimensional echocardiographic study. Am J Cardiol 1982;49:1120–6.
4. Jugdutt BI, Warnica JW. Intravenous nitroglycerin therapy to limit myocardial infarct size, expansion, and complications. Circulation 1988;78:906–19.
5. Weisman HF, Bush DE, Mannisi JA, Weisfeldt ML, Healy B. Cellular mechanisms of myocardial infarct expansion. Circulation 1988;78:186–201.
6. Mitchell GF, Lamas GA, Vaughan DE, Pfeffer MA. Left ventricular remodeling in the year after first anterior myocardial infarction. J Am Coll Cardiol 1992;19:1136–44.
7. Kramer CM, Lima JAC, Reichek N, et al. Regional function within noninfarcted myocardium during left ventricular remodeling. Circulation 1993;88:1279–88.
8. Olivetti G, Capasso JM, Meggs LG, Sonnenblick EH, Anversa P. Cellular basis of chronic ventricular remodeling after myocardial infarction in rats. Circ Res 1991;68:856–69.
9. Melillo G, Lima JAC, Judd RM, Goldschmidt-Clermont PJ, Silverman HS. Intrinsic myocyte dysfunction and tyrosine kinase pathway activation underlie the impaired wall thickening of adjacent regions during postinfarct left ventricular remodeling. Circulation 1996;93:1447–58.
10. Zerhouni E, Parrish D, Rogers WJ, Yang A, Shapiro EP. Human heart: tagging with MR imaging—a method for noninvasive measurement of myocardial motion. Radiology 1988;169:59–64.
11. Axel L, Dougherty L. MR imaging of motion with spatial modulation of magnetization. Radiology 1989;171:841–5.
12. Kramer CM, Rogers WJ, Theobald T, Power TP, Petruolo S, Reichek N. Remote noninfarcted region dysfunction soon after first anterior myocardial infarction: a magnetic resonance tagging study. Circulation 1996;94:660–6.
13. White HD, Norris RM, Brown MA, Brandt PWT, Whitlock RML, Wild CJ. Left ventricular end-systolic volume as the major determinant of survival after recovery from myocardial infarction. Circulation 1987;76:44–51.
14. Pfeffer MA, Pfeffer JM, Steinberg C, Finn P. Survival after an experimental myocardial infarction: beneficial effects of long-term therapy with captopril. Circulation 1985;72:406–12.
15. Pfeffer MA, Braunwald E, Moye LA, et al. Effect of captopril on mortality and morbidity in patients with left ventricular dysfunction after myocardial infarction. N Engl J Med 1992;327:669–77.
16. The Acute Infarction Ramipril Efficacy (AIRE) Study Investigators. Effect of ramipril on mortality and morbidity of survivors of acute myocardial infarction with clinical evidence of heart failure. Lancet 1993;342:821–8.
17. Ambiosioni E, Borghi C, Magnani B, for the Survival of Myocardial Infarction Long-term Evaluation (SMILE) Study Investigators. The effect of the angiotensin-converting enzyme inhibitor zofenopril on mortality and morbidity after anterior myocardial infarction. N Engl J Med 1995;332:80–5.
18. Holmes JW, Yamashita H, Waldman LK, Covell JW. Scar remodeling and transmural deformation after infarction in the pig. Circulation 1994;90:411–20.
19. Picard MH, Wilkins GT, Ray PA, Weyman AE. Natural history of left ventricular size and function after acute myocardial infarction. Circulation 1990;82:484–94.
20. St. John Sutton M, Pfeffer MA, Plappert T, et al. Quantitative two-dimensional echocardiographic measurements are major predictors of adverse cardiovascular events after acute myocardial infarction. Circulation 1994;89:68–75.
21. Touchstone DA, Beller GA, Nygaard TW, Tedesco C, Kaul S. Effects of successful intravenous reperfusion therapy on regional myocardial function and geometry in man: a tomographic assessment using two-dimensional echocardiography. J Am Coll Cardiol 1989;13:1506–13.
22. Penco M, Romano S, Agati L, et al. Influence of reperfusion induced by thrombolytic treatment on natural history of left ventricular regional motion abnormality in acute myocardial infarction. Am J Cardiol 1993;71:1015–20.
23. Hirose K, Reed JE, Rumberger JA. Serial changes in left and right ventricular systolic and diastolic dynamics during the first year after an index left ventricular Q wave myocardial infarction. J Am Coll Cardiol 1995;25: 1097–1104.
24. Jeremy RW, Allman KC, Bautovitch G, Harris PJ. Patterns of left ventricular dilation during the six months after myocardial infarction. J Am Coll Cardiol 1989;13:304–10.
25. Rumberger JA, Behrenbeck T, Breen JR, Reed JE, Gersh BJ. Nonparallel changes in global left ventricular chamber volume and muscle mass during the first year after transmural myocardial infarction in humans. J Am Coll Cardiol 1993;21:673–82.
26. Lee H, Eisenberg MJ, Schiller NB. Serial assessment of left ventricular function after myocardial infarction. Am Heart J 1995;130:999–1002.
27. Braunwald E, Kloner RA. The stunned myocardium: prolonged, postischemic ventricular dysfunction. Circulation 1982;66:1146–9.
28. Kramer CM, Ferrari VA, Rogers WJ, et al. Angiotensin converting enzyme inhibition limits adjacent noninfarcted region dysfunction during left ventricular remodeling. J Am Coll Cardiol 1996;27:211–7.
29. Uren NG, Crake T, Lefroy D, de Silva R, Davies G, Maseri A. Reduced coronary vasodilator function in infarcted and normal myocardium after myocardial infarction. N Engl J Med 1994;331:222–7.
30. Reichek N, Wilson J, St. John Sutton M, Plappert TA, Goldberg S, Hirshfeld JW. Noninvasive determination of left ventricular end-systolic stress: validation of the method and initial application. Circulation 1982;65:99–108.
31. Olivetti G, Capasso JM, Sonnenblick EH, Anversa P. Side-to-side slippage of myocytes participates in ventricular wall remodelling acutely after myocardial infarction in rats. Circ Res 1990;67:23–34.
32. Rouleau J-L, Packer M, Moye L, et al. Prognostic value of neurohumoral activation in patients with an acute myocardial infarction: effect of captopril. J Am Coll Cardiol 1994;24:583–91.
33. Gaudron P, Eilles C, Kugler I, Ertl G. Progressive left ventricular dysfunc-

tion and remodeling after myocardial infarction: potential mechanisms and early predictors. Circulation 1993;87:755–63.
34. Fletcher PJ, Pfeffer JM, Pfeffer MA, Braunwald E. Left ventricular diastolic pressure–volume relations in rats with healed myocardial infarction. Circ Res 1981;49:618–26.
35. Chareonthaitawee P, Christian TF, Hirose K, Gibbons RJ, Rumberger JA. Relation of initial infarct size to extent of left ventricular remodeling in the year after acute myocardial infarction. J Am Coll Cardiol 1995;25:567–73.
36. Rehr RB, Malloy CR, Filipchuk NG, Peshock RM. Left ventricular volumes measured by MR imaging. Radiology 1985;156:717–9.
37. Sobel BE, Breshnahan GF, Shell WE, Yoder RD. Estimation of infarct size in man and its relation to prognosis. Circulation 1972;46:640–8.
38. Roberts R, Henry PD, Sobel BE. An improved basis for enzymatic estimation of infarct size. Circulation 1975;52:743–54.
39. Vatner SF, Baig H, Manders WT, Maroko PR. Effects of coronary artery reperfusion on myocardial infarct size calculated from creatine kinase. J Clin Invest 1978;61:1048–56.
40. Kramer CM, Rogers WJ, Theobald T, Power TP, Petruolo S, Reichek N. MR assessment of global structure, regional function, and infarct artery patency during left ventricular remodeling after anterior myocardial infarction [abstract]. Proc Soc Magn Res 1995;1:338.
41. White HD, Cross DB, Elliott JM, Norris RM, Yee TW. Long-term prognostic importance of patency of the infarct-related coronary artery after thrombolytic therapy for acute myocardial infarction. Circulation 1994;89:61–7.
42. Lamas GA, Flaker GC, Mitchell G, et al. Effect of infarct artery patency on prognosis after acute myocardial infarction. Circulation 1995;92:1101–9.
43. Meijer A, Verheugt FWA, van Eenige MJ, Werter CJPA. Left ventricular function at 3 months after successful thrombolysis: impact of reocclusion without reinfarction on ejection fraction, regional function, and remodeling. Circulation 1994;90:1706–14.
44. Pfeffer MA, Greaves SC, Arnold JMO, et al. Early versus delayed angiotensin-converting enzyme inhibition therapy in acute myocardial infarction. Circulation 1997;95:2643–51.